

Analysis of scale-free networks based on a threshold graph with intrinsic vertex weights

Naoki Masuda,^{1,2} Hiroyoshi Miwa,³ and Norio Konno⁴

¹*Laboratory for Mathematical Neuroscience, RIKEN Brain Science Institute,*

2-1, Hirosawa, Wako, Saitama, 351-0198 Japan

²*Aihara Complexity Modelling Project, ERATO, JST,*

3-23-5, Uehara, Shibuya, Tokyo, 151-0064 Japan

³*Department of Informatics, School of Science and Technology,*

Kwansei Gakuin University, 2-1, Gakuen, Sanda, Hyogo, 669-1337 Japan

⁴*Faculty of Engineering, Yokohama National University,*

79-5, Tokiwadai, Hodogaya, Yokohama, 240-8501 Japan

(Dated: Received 29 March 2004)

Many real networks are complex and have power-law vertex degree distribution, short diameter, and high clustering. We analyze the network model based on thresholding of the summed vertex weights, which belongs to the class of networks proposed by Caldarelli *et al.* [Phys. Rev. Lett. **89**, 258702 (2002)]. Power-law degree distributions, particularly with the dynamically stable scaling exponent 2, realistic clustering, and short path lengths are produced for many types of weight distributions. Thresholding mechanisms can underlie a family of real complex networks that is characterized by cooperativeness and the baseline scaling exponent 2. It contrasts with the class of growth models with preferential attachment, which is marked by competitiveness and baseline scaling exponent 3.

PACS numbers: 89.75.Hc, 89.75.Da, 89.75.Fb

I. INTRODUCTION

Complex networks have drawn increasing interests in various disciplines. Recent studies have revealed that networks in the real world are far from fairly regular or totally random. Particularly, real networks have small average shortest path length and high clustering at

the same time, whereas conventional graphs such as lattices, trees, or the original random graphs are not equipped with these properties at the same time [1, 2].

The average path length is denoted by L , and it more or less characterizes the diameter of the graph. The average of the shortest path length over all the pairs of vertices defines L . The clustering property can be locally evaluated by the vertex-wise clustering coefficient, which is the number of connected triangles containing the vertex in question, normalized by the maximal number of possible triangles. If the vertex degree, or the number of edges emanating from a vertex, is k , the normalization constant becomes $k(k-1)/2$. The clustering coefficient C of the whole graph is the local clustering coefficient averaged over all the vertices. Watts and Strogatz proposed the small-world networks that simultaneously realize large C and small L [1]. However, the small-world networks are short of the scaling property of vertex degree distribution denoted by $p(k)$. Indeed, not all but many real networks satisfy $p(k) \propto k^{-\gamma}$ typically with $2 < \gamma < 3$ [2]. Then, Barabási and Albert (BA) developed the network model, which dynamically generates scale-free networks with $\gamma = 3$ [2, 3]. The fundamental devices in the BA model are the network growth and the preferential attachment; vertices are added one after another to the network, and edges are more prone to be connected to vertices with larger k . Various scale-free networks including extensions of the BA model, such as networks with dynamic edge rewiring [4, 5], those with nonlinear preferential attachment [6], those with weights on edges [7], the fitness model [8], and the hierarchically and deterministically growing models [9, 10, 11, 12, 13] have been proposed. These models largely yield more flexible values of γ , which is restricted to 3 in the original BA construction. Furthermore, modifications to reinforce the clustering property, which the BA model lacks, have also been done. A simple solution is to embed a triangle-generating protocol into the BA model [14, 15]. Introduction of a node deactivation procedure also enhances clustering [16, 17]. Yet another solution is appropriately designed versions of the hierarchical models mentioned above [10, 12, 13]. In short, large C , small L , and scale-free $p(k)$ can be simultaneously realized by the modified BA models or by the hierarchical construction. Both models rely on the combined effects of network growth and the preferential attachment, although preferential attachment is not explicitly implemented in the hierarchical networks.

Nevertheless, every network is not apparently growing. Networks can experience structural changes that are relatively much faster than network growth or aging processes. In

economical networks of companies, friendship networks, peer-to-peer (P2P) networks, and networks of computer programs, for example, it seems natural that agents change their connectivity without significant entries or leaves of members. Therefore, there has been a need for developing a nongrowing algorithm to generate realistic networks. In this regard, Caldarelli *et al.* proposed a class of networks whose connections are determined by interactions of vertices that are endowed with intrinsic weights [18, 19, 20]. The vertex weight is considered as a type of fitness [8, 18, 21, 22, 23], which describes the propensity of vertices to gain edges. It can be interpreted as money, social skills, or personal influence in social networks, activeness, the value of information attached to a vertex, concentration or mass of some ingredients in chemical or biological networks, or the vertex degree itself. Surprisingly, scale-free topology spontaneously emerges even with weight distributions without power laws [18, 20].

In this paper, we analyze a subclass of their model that is based on a deterministic thresholding mechanism. The connectivity between a pair of vertices is determined by whether the sum of the weights of the pair exceeds a given threshold. Actually, this class of networks is equivalent to the threshold graph in the graph theoretical context [24], and we also discuss its consequence.

Despite the stochasticity and certain continuity in the real world, thresholding that is more or less “hard” is often observed. Although the correspondence to our framework is not perfect, a common form of thresholding is that an agent on a vertex determines its action or state based on the number of neighbors taking a specific state. For example, propagation of riots, fashions, and innovations are considered to be equipped with thresholding mechanisms [25]. These phenomena have been simulated by dynamic models, such as the threshold model for social decision [25], the minority games [26], the threshold voter models, and the threshold contact processes [27].

In this paper, we show that a baseline power law $p(k) \propto k^{-\gamma}$ with $\gamma = 2$ rather than one with $\gamma = 3$ [3] dominates this class of models and explore its cause and consequence. In Sec. II, we follow Refs. [18, 20] to explain the network model, and calculate fundamental quantities such as $p(k)$, C , and the measure for degree correlation. The results in Sec. II are applied to various weight distribution functions in Sec. III, extending the results for the exponential distributions in Refs. [18, 20]. Consequently, we find that the power law is observed for a wide class of weight distributions. In Sec. IV, we argue that the power law

with $\gamma = 2$ is rather ubiquitous in the sense that it is a unique stable degree distribution when a network evolves without growth.

II. MODEL

Let us start with a set of n vertices $V = \{v_1, v_2, \dots, v_n\}$. As introduced in Refs. [18, 20], we assign to each v_i ($1 \leq i \leq n$) a weight $w_i \in \mathbf{R}$ that is taken randomly and independently distributed as specified by a given probability distribution function $f(w)$ on \mathbf{R} . The weight quantifies the potential for the vertex to be linked to other vertices [8, 18]. We assume that the weight permits additive operation. Actually, the multipliable weights [18, 20, 21, 23] can be easily reduced to the additive ones by taking the logarithm of w . Let

$$F(w) = \int_{-\infty}^w f(w') dw' \quad (1)$$

be the cumulative distribution function, satisfying $\lim_{w \rightarrow -\infty} F(w) = 0$ and $\lim_{w \rightarrow \infty} F(w) = 1$. The set of edges E is defined by the thresholding rule with threshold θ : $E = \{(v_i, v_j); w_i + w_j \geq \theta, i \neq j\}$. We focus on this specific case of more general framework [18, 20]. This renders more mathematical analysis and allows us to explore the consequence of vertex interactions based on intrinsic weights. The degree distribution $p(k)$, where $0 \leq k < n$ is the vertex degree, is readily calculated with the use of continuum approximation corresponding to the thermodynamic limit ($n \rightarrow \infty$). However, we confine ourselves to a finite n , and the limit $n \rightarrow \infty$ should be understood as approximation. Putting the upper limit of k equal to n instead of $n - 1$, we obtain

$$k = n \int_{\theta-w}^{\infty} f(w') dw' = n [1 - F(\theta - w)], \quad (0 \leq k \leq n) \quad (2)$$

and

$$p(k) = f(w) \frac{dw}{dk} = \frac{f\left(\theta - F^{-1}\left(1 - \frac{k}{n}\right)\right)}{n f\left(F^{-1}\left(1 - \frac{k}{n}\right)\right)}. \quad (3)$$

Because of the one-to-one correspondence between k and w represented by Eq. (2), the vertex-wise cluster coefficient depends only on k , which simplifies the analysis. We denote it by $C(k)$, and the scaling law $C(k) \propto k^{-1}$ is often observed in real and modeled networks [10, 12, 13, 15, 16, 17, 28]. The clustering coefficient of the entire graph is given by $C = \int_0^\infty C(k) p(k) dk$. To calculate $C(k)$ [20], let us consider a vertex v

with degree $k = n[1 - F(\theta - w)]$. The density of the number of neighbors with degree $k' = n[1 - F(\theta - w')]$ becomes $f(w')$ if $w' \geq \theta - w$ and 0 otherwise. With such a neighbor denoted by v' , the number of connected triangles comprising v , v' and another neighbor of v is obtained as follows. When $k' \geq k$, a new neighbor of v is also a neighbor of v' because $w' \geq w$. The number of triangles in this case is

$$(n - 2)[1 - F(\theta - w)] \cong n[1 - F(\theta - w)] = k. \quad (4)$$

When $k' < k$, we have

$$\int_{\theta-w'}^{\infty} n f(w'') dw'' = n[1 - F(\theta - w')] \quad (5)$$

triangles. We obtain $C(k)$ by the sum of Eqs. (4) and (5) that is weighted by the degree distribution. The normalization is given by dividing it by $k(k-1)/2$ and by another factor of 2, as each triangle is counted twice. Consequently, we have for $w > \theta/2$, or $k > n[1 - F(\theta/2)]$

$$\begin{aligned} C(k) &= \frac{1}{2} \frac{1}{k(k-1)/2} \left\{ \int_w^{\infty} k f(w') dw' + \int_{\theta-w}^w n[1 - F(\theta - w')] f(w') dw' \right\} \\ &= \left\{ -1 + 2\frac{k}{n} + \left(1 - \frac{k}{n}\right) F\left(\theta - F^{-1}\left(1 - \frac{k}{n}\right)\right) \right. \\ &\quad \left. - \int_{n[1-F(\theta-F^{-1}(1-k/n))]}^k \left(1 - \frac{k'}{n}\right) p(k') dk' \right\} / (k/n)^2. \end{aligned} \quad (6)$$

When $w \leq \theta/2$ or $k \leq n[1 - F(\theta/2)]$, we simply end up with

$$C(k) = 1. \quad (7)$$

The vertices with $C(k) = 1$ forms the peripheral part of the network that is connected to the cliquish core with smaller $C(k)$, as schematically depicted in Fig. 1. The core consists of the vertices with $w \geq \theta/2$, and it is similar to the winner-take-all phenomenon found in growing network models [6, 8]. However, more than a single winners are allowed in this model. This core-peripheral separability is a rigorous property of the threshold graph [24]. It is also consistent with the property of real networks that $C(k)$ saturates for small k [12, 13] and that vertices in the core are densely connected [29].

Regarding the network size, real networks are small with L proportional to $\ln n$ or even less [1, 2, 3]. Our network has $L \leq 2$ as far as it is free from isolated vertices. This is because any pair of vertices can be connected by a path of length 2 passing a vertex with a sufficiently large weight is in the cliquish part (see Fig. 1). One might ascribe this ultrasmallness to

the fact that the mean degree is of the order of n , indicating too many edges per vertex. However, the mean degree can be kept finite by scaling θ according to the increase in n , as discussed in Sec. III A. It turns out that this modification does not change L .

The correlation between the degrees of adjacent vertices also characterizes networks [2]. Actually, degree correlation can be positive or negative depending on the type of network, as measured for real data using the degree of assortativity [30]. Here we explain a simpler quantity to gain insight into the degree correlation [5, 16, 17], which was first analyzed in Ref. [20] for the present type of network model. We denote by k_2 the sum of the degrees of v 's neighbors, which has degree k . If the degree is uncorrelated, k_2/k , or the average degree of the neighbors, is independent of v or k . For the threshold model, we derive

$$\begin{aligned} k_2 &= \int_{\theta-w}^{\infty} n f(w') n [1 - F(\theta - w')] dw' \\ &= n^2 \left\{ \frac{k}{n} - \int_{n[1-F(\theta-F^{-1}(1-k/n))]}^n \left(1 - \frac{k'}{n} \right) p(k') dk' \right\}. \end{aligned} \quad (8)$$

Accordingly,

$$\frac{k_2}{k} = n \left\{ 1 - \frac{1}{k} \int_{n[1-F(\theta-F^{-1}(1-k/n))]}^n (n - k') p(k') dk' \right\}, \quad (9)$$

which generally depends on k .

III. EXAMPLES

In this section, we calculate the quantities introduced in Sec. II for some weight distributions $f(w)$.

A. Exponential distribution

Let us begin with recapitulating the case of exponential weight distribution with deterministic thresholding [18, 20]. We set

$$f(w) = \lambda e^{-\lambda w} \quad (0 \leq w). \quad (10)$$

Assuming $\theta > 0$ so that the generated networks are not trivial, for $w < \theta$, combining Eqs. (3) and (10) results in

$$p(k) = \frac{n e^{-\lambda \theta}}{k^2} \quad (n e^{-\lambda \theta} \leq k \leq n). \quad (11)$$

The scale-free distribution $p(k) \propto k^{-2}$ appears from random weights whose distribution has nothing to do with power law, which is a main claim of Ref. [18]. A total of $\int_{\theta}^{\infty} n f(w) dw = ne^{-\lambda\theta}$ vertices are condensated at $k = n$ and form a core [18, 20]. In general, this sort of condensation occurs when $f(w)$ has a lower cutoff. However, the number of vertices with $k = n$ can be made arbitrarily small by setting large $\lambda\theta$, and this feature is not so essential. We numerically simulate a network with $n = 50000$, which is fixed throughout the paper, $\lambda = 1$, and $\theta = 10$. Setting $\lambda = 1$ does not cause the loss of generality because only the multiple of λ and θ appears in Eq. (11) and the following quantities [Eqs. (12) and (15)]. Figure 2(a) shows that numerical results (crosses) are predicted by Eq. (11) (lines) sufficiently well [18, 20]. In regard to clustering, Eq. (6) yields

$$C(k) = \begin{cases} 1 & (ne^{-\lambda\theta} \leq k \leq ne^{-\lambda\theta/2}) \\ \frac{n^2}{k^2} e^{-\lambda\theta} \left(1 + \lambda\theta + 2 \ln \frac{k}{n}\right) & (ne^{-\lambda\theta/2} < k \leq n) \end{cases} \quad (12)$$

which agrees with the numerical results in Fig. 2(b) (crosses) (originally derived in Ref. [20]). Equation (12) shows that $C(k)$ nearly decays according to the power law with exponent 2. However, analysis of real networks, such as metabolic networks [12], actor networks, semantic networks, world wide webs, and the Internet [13], suggests $C(k) \propto k^{-1}$, which is also supported by some models [5, 10, 12, 13, 15, 16, 17, 28]. For this particular example, we have a larger scaling exponent. Actually, the general power-law form $C(k) \propto k^{-\gamma'}$ ($\gamma' > 0$) is also reported in model studies [5, 13, 15] and in data analysis [5]. The clustering coefficient of the whole network is

$$C = \int_{ne^{-\lambda\theta}}^n C(k) p(k) dk = 1 - \frac{4}{9} e^{-\lambda\theta/2} - \frac{5 + 3\lambda\theta}{9} e^{-2\lambda\theta}. \quad (13)$$

In real networks, the average vertex degree denoted by $\langle k \rangle$ is independent of n on a large scale [1, 2, 3]. Since

$$\langle k \rangle = e^{-\lambda\theta} (n + \lambda\theta), \quad (14)$$

finite $\langle k \rangle$ is maintained by setting $\theta \cong \lambda^{-1} \ln n$. With this scaling of θ , our model produces a finite value of C that does not decay to 0 in the limit $n \rightarrow \infty$. This result agrees with real data [2], and C is actually nonvanishing for more general $f(w)$.

Using Eq. (9), the average degree of neighbors becomes, as shown in Ref. [20],

$$\frac{k_2}{k} = \frac{n^2 e^{-\lambda\theta}}{k} \left(1 + \lambda\theta + \ln \frac{k}{n}\right). \quad (15)$$

Since Eq. (15) is decreasing in k , the network is disassortative [30] with negative degree correlation, which is a property shared by some scale-free network models [5, 16, 17] and some social and biological networks [2, 5, 30]. More intuitively, disassortativity of our model is a natural consequence of the core-peripheral structure. Equation (15) and Fig. 2(c) (crosses and solid lines) show that there is an approximate scaling relation $k_2/k \propto k^{-1}$ [17].

B. Logistic distribution

The logistic distribution is often used, for example, in statistics and economics. Except the discrepancy in the asymptotic behavior, it can be used as a more or less appropriate substitute for the Gaussian distribution. The logistic distribution is more tractable because it has an analytic form of $F(w)$. For a given $\beta > 0$, the logistic distribution is defined by

$$f(w) = \frac{\beta e^{-\beta w}}{(1 + e^{-\beta w})^2}, \quad (16)$$

With

$$F(w) = \frac{1}{1 + e^{-\beta w}}, \quad (w \in \mathbf{R}) \quad (17)$$

$$F^{-1}(x) = -\frac{1}{\beta} \ln \left(\frac{1}{x} - 1 \right), \quad (18)$$

$$k = \frac{ne^{\beta(w-\theta)}}{1 + e^{\beta(w-\theta)}}, \quad (19)$$

$$w = \theta + \frac{1}{\beta} \ln \frac{k}{n-k}. \quad (20)$$

applied to Eq. (3), we obtain

$$p(k) = \frac{ne^{-\beta\theta}}{k^2 \left(1 + e^{-\beta\theta} \frac{n-k}{k} \right)^2} \quad (0 \leq k \leq n). \quad (21)$$

The power law $p(k) \propto k^{-2}$ is again manifested as k approaches n . If $1 \ll [(n-k)/k]e^{-\beta\theta}$, k is relatively small, and $p(k) \cong ne^{\beta\theta}/(n-k)^2$ does not strongly depend on k . The crossover from this regime to the power-law regime, which is found in real data [12, 13] and derived by scaling ansatz theory [15], occurs around $1 \cong [(n-k)/k]e^{-\beta\theta}$, or $k \cong [n/(e^{\beta\theta} + 1)]$. A larger value of $\beta\theta$ provides a wider range of k in which the power law holds. In this range, Eq. (16) is of course approximated by the exponential distribution represented by Eq. (10) with $\beta = \lambda$. For k small relative to $n/(e^{\beta\theta} + 1)$, $f(w)$, with a correspondingly small w , does

not decay exponentially or even monotonically. Therefore, when k is small, the number of vertices with degree k is not large enough to support the power law.

We compare in Figs. 2(a) the numerical results for $\theta = 6$ (open squares) and $\theta = 10$ (open circles) with the corresponding theoretical results in Eq. (21) (dotted lines). We have set $\beta = 1$ without losing generality for the same reason as in Sec. III A. The effect of θ on the position of crossover is clear in the figure. Since the integrals in Eqs. (6) and (9) cannot be explicitly calculated, numerically evaluated $C(k)$ and k_2/k with the same parameter values are shown in Figs. 2(b) and 2(c), respectively. Similar to the case of the exponential distribution, the crossover from the plateau to the power law is observed for $C(k)$ with the same scaling exponent $C(k) \propto k^{-2}$. Also with regard to the degree correlation, $k_2/k \propto k^{-1}$ approximately holds except for small k .

C. Gaussian distribution

The Gaussian distribution can be a standard null hypothesis on the weight distribution. Since it does not have the analytical form of $F^{-1}(x)$, we perform straightforward numerical simulations with $\theta = 6$ and $\theta = 10$ to examine $p(k)$, $C(k)$, and k_2/k . The Gaussian distribution is assumed to have mean 0 and standard deviation 1.7 to roughly approximate the logistic distribution with $\beta = 1$, which has been used in Sec. III B. In spite of different asymptotic decay rates of $f(w)$, Fig. 2 indicates that $p(k)$, $C(k)$, and k_2/k for the Gaussian distribution do not differ so much from those for the logistic distribution, disregarding the crossover points. This implies a rather universal existence of power law behavior, which is discussed in more detail in Sec. IV.

D. Pareto distribution

The Pareto distribution, which is equipped with an inherent power law, is often observed in, for example, distributions of capitals and company sizes [31]. It is defined by

$$f(w) = \frac{a}{w_0} \left(\frac{w_0}{w} \right)^{a+1} \quad (w \geq w_0), \quad (22)$$

where $a > 0$ and $w_0 > 0$. Nontrivial networks form if we choose $\theta > 2w_0$. We obtain

$$F(w) = 1 - \left(\frac{w_0}{w} \right)^a \quad (w \geq w_0), \quad (23)$$

$$F^{-1}(x) = \frac{w_0}{(1-x)^{1/a}}. \quad (24)$$

When $w \leq \theta - w_0$, it is straightforward to derive

$$k = n \left(\frac{w_0}{\theta - w} \right)^a, \quad \left(n \left(\frac{w_0}{\theta - w_0} \right)^a \leq k < n \right) \quad (25)$$

$$w = \theta - \left(\frac{n}{k} \right)^{1/a} w_0, \quad (26)$$

$$p(k) = \frac{n^{1/a}}{\left(\frac{\theta}{w_0} k^{1/a} - n^{1/a} \right)^{a+1}}. \quad (27)$$

A total of

$$\int_{\theta-w_0}^{\infty} n f(w) dw = n \left(\frac{w_0}{\theta - w_0} \right)^a \quad (28)$$

vertices with $w \geq \theta - w_0$ are condensated at $k = n$. When $n(w_0/\theta)^a \ll k < n$, $p(k)$ can be approximated by a power law

$$p(k) \cong \left(\frac{w_0}{\theta} \right)^{a+1} n^{1/a} k^{-(a+1)/a}. \quad (29)$$

By modulating a , we can produce a scale-free $p(k)$ with arbitrary $\gamma = (a+1)/a > 1$. An observed γ in turn serves to estimate a and $f(w)$, which may underly, for example, fractal dynamics of economical quantities, as well as network formation. The scaling exponent for $p(k)$ differs from that for $f(w)$, and a faster decay of $f(w)$ with a larger a yields a slower decay of $p(k)$. Numerical results for $p(k)$ are shown in Fig. 3(a) with $w_0 = 1$. We set $(a, \theta) = (0.5, 100)$ (open squares) and $(0.5, 500)$ (open circles), yielding $\gamma = 3$, and $(a, \theta) = (1, 100)$ (closed squares) and $(1, 500)$ (closed circles), resulting in $\gamma = 2$. The results are consistent with the theoretical prediction based on Eq. (27) (solid lines) and also with Eq. (29) (dotted lines).

Substituting Eqs. (23), (24), and (27) into Eqs. (6), (7), and (9), respectively, yields

$$\begin{aligned} C(k) &= \frac{n}{k} + \left(\frac{n}{k} - \frac{n^2}{k^2} \right) \left(\frac{w_0}{\theta - w_0 \left(\frac{n}{k} \right)^{1/a}} \right)^a - \frac{n^2 a}{k^2} \left(\frac{w_0}{\theta} \right)^a \int_{\theta/[\theta - w_0(n/k)^{1/a}]}^{(k/n)^{1/a}(\theta/w_0)} \frac{x^{a-1} - \left(\frac{w_0}{\theta} \right)^a x^{2a-1}}{(x-1)^{a+1}} dx \\ &= \frac{n}{k} \left(\frac{w_0}{\theta - w_0 \left(\frac{n}{k} \right)^{1/a}} \right)^a + \frac{n^2 a}{k^2} \left(\frac{w_0}{\theta} \right)^{2a} \int_{(n/k)^{1/a}(w_0/\theta)}^{1-(n/k)^{1/a}(w_0/\theta)} y^{-a} (1-y)^{-a-1} dy, \\ &\quad \left(k > n \left(\frac{2w_0}{\theta} \right)^a \right), \end{aligned} \quad (30)$$

$$C(k) = 1, \quad \left(n \left(\frac{w_0}{\theta - w_0} \right)^a \leq k \leq n \left(\frac{2w_0}{\theta} \right)^a \right) \quad (31)$$

and

$$\begin{aligned} \frac{k_2}{k} &= n \left\{ 1 - \frac{na}{k} \left(\frac{w_0}{\theta} \right)^a \int_{\theta/[\theta - w_0(n/k)^{1/a}]}^{\theta/w_0} \frac{x^{a-1} - \left(\frac{w_0}{\theta} \right)^a x^{2a-1}}{(x-1)^{a+1}} dx \right\} \\ &= \frac{n^2}{k} \left(\frac{w_0}{\theta - w_0} \right)^a + \frac{n^2 a}{k} \left(\frac{w_0}{\theta} \right)^{2a} \int_{w_0/\theta}^{1 - (n/k)^{1/a} (w_0/\theta)} y^{-a} (1-y)^{-a-1} dy, \end{aligned} \quad (32)$$

where we set $y = x^{-1}$. The integral in Eq. (30) is nonnegative and does not depend so much on k when k tends large. Therefore, $C(k) \propto k^{-1}$ is expected based on the first term, which is consistent with the numerical results for k larger than the crossover value $k \cong n(2w_0/\theta)^a$ [Fig. 3(b)]. The scaling law $C(k) \propto k^{-1}$, as opposed to $C(k) \propto k^{-2}$ for the exponential $f(w)$, rather agrees with real data [12, 13].

Similarly, Eq. (32) and the simulation results shown in Fig. 3(c) suggest $k_2/k \propto k^{-1}$ for a sufficiently large k . Equations (30) and (32) show that the scaling exponents of both $C(k)$ and k_2/k do not depend on γ or a .

E. Cauchy distribution

For the Cauchy distribution

$$f(w) = \frac{1}{\pi(1+w^2)} \quad (w \in \mathbf{R}), \quad (33)$$

we obtain

$$F^{-1}(x) = \tan \frac{\pi}{2} (2x - 1), \quad (34)$$

$$w = \theta - \tan \frac{\pi}{2} \left(1 - \frac{2k}{n} \right), \quad (35)$$

$$p(k) = \frac{1}{n} \frac{1 + \tan^2 \frac{\pi}{2} \left(1 - \frac{2k}{n} \right)}{1 + \left(\theta - \tan \frac{\pi}{2} \left(1 - \frac{2k}{n} \right) \right)^2} \quad (0 \leq k \leq n). \quad (36)$$

Numerically obtained $p(k)$, $C(k)$, and k_2/k together with Eq. (36) are shown in Fig. 4 for $\theta = 100$ (open squares) and for $\theta = 500$ (open circles). According to Eq. (36), the monotonicity of $p(k)$ is marred because $p(0) = p(n) = 1/n$. A particular choice of $\theta = 0$ even gives rise to the uniform $p(k)$. For general θ , however, $p(k)$ has the unique maximum and minimum between $k = 0$ and $k = n$ as shown in Fig. 4(a) by solid lines. Existence of the characteristic vertex degree corresponding to the peak of $p(k)$ is a feature shared by random, regular and small-world networks [1, 2]. The peak appears because of the unimodality of

$f(w)$, which yields the plateaus of $p(k)$ in the case of the logistic and Gaussian distributions (see Secs. III B and III C). Nonetheless, as for the Pareto distribution with $a = 1$, which has the same asymptotics $f(w) \propto w^{-2}$ as the Cauchy distribution, approximate power laws with $\gamma = 2$ are observed for intermediate values of k .

The one-sided Cauchy distribution on the half line facilitates a fairer comparison with the Pareto distribution that also has the lower cutoff of w . We define the one-sided Cauchy distribution by

$$f(w) = \frac{2}{\pi(1+w^2)} \quad (w \geq 0). \quad (37)$$

Then it holds that $F^{-1}(x) = \tan(\pi/2)x$ and

$$p(k) = \frac{2}{n} \frac{1 + \tan^2 \frac{\pi}{2} \left(1 - \frac{k}{n}\right)}{1 + \left(\theta - \tan \frac{\pi}{2} \left(1 - \frac{k}{n}\right)\right)^2} \quad (0 \leq k \leq n). \quad (38)$$

Figure 4(a) shows the numerical results for $p(k)$ with $\theta = 100$ (closed squares) and $\theta = 500$ (closed circles), accompanied by the prediction by Eq. (38) (dotted lines). The approximate power law holds even for k close to n , which contrasts with the case of the standard Cauchy distribution. The behavior of $C(k)$ and k_2/k shown in Figs. 4(b) and 4(c), respectively, resembles that for the Pareto and standard Cauchy distributions. In Secs. III A and III B, we have inspected consequences of using exponential $f(w)$ and logistic $f(w)$. Including the comparison between the Pareto and Cauchy distributions examined here, effect of a lower cutoff of $f(w)$ does not seem so prominent.

IV. WHY POWER LAW WITH $\gamma = 2$?

The power law of $p(k)$ with $\gamma = 2$ seems universal for thresholding mechanisms not only because a wide class of $f(w)$ generates it but also owing to its stability. To be more specific, weights can be the vertex degrees themselves, as is implied by the BA model. Indeed, k can represent how central or influential a node is [22]. Then let us iterate our construction algorithm to simulate an evolving but not growing network with dynamic $f(w)$ and $p(k)$. Let us simulate a dynamical network with $n = 50000$. Initially, w is uniformly distributed on $[0, 1]$, and the thresholding algorithm determines k . Then we set $w = k/n + \xi$, where ξ is the Gaussian white noise with standard deviation $\sigma = 0.2$, and iterate the dynamics. The numerical results are shown in Fig. 5 with $\theta = 1$. In the early stages [crosses in Fig. 5(a)],

k is distributed more or less uniformly since a uniform $f(w)$ yields a uniform $p(k)$ just accompanied by a singularity at $k = 0$ or $k = n$, which is easily checked with Eq. (3). As the iteration goes on, however, $p(k)$ converges to a power law with $\gamma = 2$. Similarly, $C(k) \propto k^{-1}$ and $k_2/k \propto k^{-1}$ are eventually realized as shown in Figs. 5(b) and 5(c). Although θ too far from 1 or excessively small σ results in a complete or totally disconnected network, $p(k) \propto k^{-2}$ emerges robustly against changes in $\theta \geq 1$ and $\sigma > 0.15$ unless noise is not extremely large.

By the analogy of the Pareto case, if a power law with $\gamma \neq 2$ is obtained, γ will be transformed by the map $\gamma = a + 1 \rightarrow \gamma = (a + 1)/a$, namely, $\gamma \rightarrow \gamma/(\gamma - 1)$. This map has a unique positive fixed point $\gamma = 2$. Actually, the map is neutrally stable at $\gamma = 2$ with eigenvalue -1 , which implies oscillation. This argument does not directly support but may underlie the emergence of $p(k) \propto k^{-2}$. In addition, $p(k)$ converges to $p(k) \propto k^{-2}$ stably with respect to the choice of initial distribution $f(w)$. It is in a striking contrast with the case of competitive growing networks with vertex weights, which generate $p(k) \propto k^{-\gamma}$ only for a limited class of weight distributions [8]. More broadly, general cooperative networks in which interactions of multiple vertices leads to interconnection [18] may have stable power laws, possibly with $\gamma \neq 2$. As an example, we can assume w of the next generation to be proportional to k^x ($x > 0$), which is often the case in real networks [22]. In this case, it is easy to show that the neutrally stable fixed point of the abovementioned map is $\gamma = 1 + \sqrt{x}$. Our model, which yields $\gamma = 2$, sets a baseline example of this class.

In terms of clustering, we have observed the discrepancy in the scaling law $C(k) \propto k^{-2}$ for the exponential, logistic, and Gaussian distributions with $C(k) \propto k^{-1}$ for the Pareto, Cauchy, and one-sided Cauchy distributions. The Pareto distribution with $a = 1$ results in $p(k) \propto k^{-2}$, which coincides with the scaling law for the exponential type of $f(w)$. It means that the consistency in $p(k)$ for different choices of $f(w)$ does not necessarily mean the consistency in network structure. The difference between the exponential tail and the power-law tail of $f(w)$ is likely to cause qualitative discrepancy in $C(k)$. On the other hand, the degree correlation behaves similarly in all the examined cases, namely, $k_2/k \propto k^{-1}$. From a dynamical point of view, $C(k)$ evolves from a general form to $C(k) \propto k^{-1}$, which is realistic [12, 13]. This scenario matches the simulated dynamics shown in Fig. 5(b). In this case, $C(k)$ is initially just large for most vertices and converges to $C(k) \propto k^{-1}$, which reflects the eventual separation of the network into the core and the peripheral part.

Boosted by the original BA models, the power law of $p(k)$ with $\gamma = 3$ has been pronounced in the first place [2, 3]. Moreover, in percolation and contact processes on scale-free networks, the critical value of the infection rate is extinguished if $\gamma \leq 3$ [32]. These results suggest relevance of the power law with $\gamma \cong 3$. However, real scale-free networks have more dispersed values of γ [2], and many models have been proposed so that γ is tunable somewhere between 2 and ∞ [4, 6, 8, 9, 10, 11, 12, 13, 14, 16, 22, 33]. In contrast, the present model with intrinsic vertex weights (also see Refs. [18, 20]) and another type of thresholding model [33] broadly yield $\gamma = 2$. We speculate that $\gamma = 2$ is another general law. In the parameter space of γ , $\gamma = 2$ as well as $\gamma = 3$ often emerges as phase transition points of network characteristics [4, 6, 10, 21, 22]. The $\gamma = 2$ law may be common to cooperative models such as those with thresholding, while the $\gamma = 3$ law underlies the competitive models represented by network growth with preferential attachment. Actually, many real networks in the scale-free regime have γ close to 2 rather than to 3 [2]. Some networks such as the world wide web, e-mail networks, language networks, and ecological networks have γ even smaller than 2 [34]. Some of these observations can be understood as small deviations from our $\gamma = 2$ law, which may be explained by proper modification of the model [18, 20], for example, by introducing stochastic thresholding [21, 23], nonlinear relations between k and w [22], or many-body interactions.

V. CONCLUSIONS

We have shown that the thresholding model, which is in the class of networks with intrinsic vertex weights, generates scale-free networks with $\gamma = 2$, large C , and small L for a broad choice of weight distributions. Even if we start with an arbitrary weight distribution, $p(k) \propto k^{-2}$ and $C(k) \propto k^{-1}$ are finally obtained. The competitive mechanisms, such as network growth with preferential attachment or hierarchical structure, are not mandatory for generating realistic networks [18]. The cooperative thresholding mechanisms also result in desired properties rather generally, and they yield somewhat different characteristics from those of growing types of networks. In addition, they allow plausible physical interpretations, have core-peripheral structure, are equipped with inhomogeneity as in real networks, and facilitate analytical calculations [18, 20].

Acknowledgments

We thank G. Caldarelli, P. De Los Rios, and A. Flammini for valuable comments and introducing us the important references. This study is supported by the Grant-in-Aid for Scientific Research, Grant-in-Aid for Young Scientists (B) (Grant No. 15700020), and the Grant-in-Aid for Scientific Research (B) (Grant No. 12440024) of Japan Society of the Promotion of Science.

- [1] D. J. Watts and S. H. Strogatz, *Nature* (London) **393**, 440 (1998).
- [2] R. Albert and A.-L. Barabási, *Rev. Mod. Phys.* **74**, 47 (2002); S. N. Dorogovtsev and J. F. F. Mendes, *Adv. Phys.* **51**, 1079 (2002); M. E. J. Newman, *SIAM Rev.* **45**, 167 (2003).
- [3] A.-L. Barabási and R. Albert, *Science* **286**, 509 (1999).
- [4] R. Albert and A.-L. Barabási, *Phys. Rev. Lett.* **85**, 5234 (2000).
- [5] A. Vázquez, R. Pastor-Satorras, and A. Vespignani, *Phys. Rev. E* **65**, 066130 (2002).
- [6] P. L. Krapivsky, S. Redner, and F. Leyvraz, *Phys. Rev. Lett.* **85**, 4629 (2000).
- [7] S. H. Yook, H. Jeong, A.-L. Barabási, and Y. Tu, *Phys. Rev. Lett.* **86**, 5835 (2001).
- [8] G. Bianconi and A.-L. Barabási, *Europhys. Lett.* **54**, 436 (2001); *Phys. Rev. Lett.* **86**, 5632 (2001).
- [9] A.-L. Barabási, E. Ravasz, and T. Vicsek, *Physica A* **299**, 559 (2001).
- [10] S. N. Dorogovtsev, A. V. Goltsev, and J. F. F. Mendes, *Phys. Rev. E* **65**, 066122 (2002).
- [11] S. Jung, S. Kim, and B. Kahng, *Phys. Rev. E* **65**, 056101 (2002).
- [12] E. Ravasz *et al.*, *Science* **297**, 1551 (2002).
- [13] E. Ravasz and A.-L. Barabási, *Phys. Rev. E* **67**, 026112 (2003).
- [14] P. Holme and B. J. Kim, *Phys. Rev. E* **65**, 026107 (2002).
- [15] G. Szabó, M. Alava, and J. Kertész, *Phys. Rev. E* **67**, 056102 (2003).
- [16] K. Klemm and V. M. Eguíluz, *Phys. Rev. E* **65**, 036123 (2002); **65**, 057102 (2002).
- [17] A. Vázquez *et al.*, *Phys. Rev. E* **67**, 046111 (2003).
- [18] G. Caldarelli, A. Capocci, P. De Los Rios, and M. A. Muñoz, *Phys. Rev. Lett.* **89**, 258702 (2002); V. D. P. Servedio, G. Caldarelli, and P. Buttà, *cond-mat/0309659* (2003).
- [19] B. Söderberg, *Phys. Rev. E* **66**, 066121 (2002).

- [20] M. Boguñá and R. Pastor-Satorras, Phys. Rev. E **68**, 036112 (2003).
- [21] F. Chung and L. Lu, Proc. Natl. Acad. Sci. U.S.A **99**, 15879 (2002).
- [22] A. Barrat, M. Barthélemy, and A. Vespignani, Phys. Rev. Lett. **92**, 228701 (2004); A. Barrat, M. Barthélemy, R. Pastor-Satorras, and A. Vespignani, Proc. Natl. Acad. Sci. U.S.A **101**, 3747 (2004).
- [23] K. -I. Goh, B. Kahng, and D. Kim, Phys. Rev. Lett. **87**, 278701 (2001); M. E. J. Newman, Phys. Rev. E **67**, 026126 (2003).
- [24] M. C. Golumbic, *Algorithmic Graph Theory and Perfect Graphs* (Academic Press, New York, 1980).
- [25] M. Granovetter, Am. J. Sociol. **83**, 1420 (1978).
- [26] W. B. Arthur, Science **284**, 107 (1999); D. Challet, M. Marsili, and R. Zecchina, Phys. Rev. Lett. **84**, 1824 (2000).
- [27] T. M. Liggett *Stochastic Interacting Systems: Contact, Voter and Exclusion Processes* (Springer-Verlag, Berlin, 1999).
- [28] M. E. J. Newman, Phys. Rev. E **68**, 026121 (2003).
- [29] S. Zhou and R. J. Mondragon, IEEE Comm. Lett. **8**, 180 (2004).
- [30] M. E. J. Newman, Phys. Rev. Lett. **89**, 208701 (2002).
- [31] M. H. R. Stanley *et al.*, Nature (London) **379**, 804 (1996); M. Marsili and Y. C. Zhang, Phys. Rev. Lett. **80**, 2741 (1998); D. H. Zanette and S. C. Manrubia, *ibid.* **79**, 523 (1998); K. Okuyama, M. Takayasu, and H. Takayasu, Physica A **269**, 125 (1999); R. L. Axtell, Science **293**, 1818 (2001).
- [32] R. Pastor-Satorras and A. Vespignani, Phys. Rev. Lett. **86**, 3200 (2001); M. E. J. Newman, Phys. Rev. E **66**, 016128 (2002); M. Boguñá, R. Pastor-Satorras, and A. Vespignani, Phys. Rev. Lett. **90**, 028701 (2003); N. Masuda, N. Konno, and K. Aihara, Phys. Rev. E, **69**, 031917 (2004).
- [33] D. Volchenkov and Ph. Blanchard, Physica A **315**, 677 (2002).
- [34] L. A. Adamic and B. A. Huberman, Science **287**, 2115a (2000); R. V. Solé and J. M. Montoya, Proc. R. Soc. London, Ser. B **268**, 2039 (2001); R. Ferrer i Cancho and R. V. Solé, *ibid.* **268**, 2261 (2001); J. M. Montoya and R. V. Solé, J. Theor. Biol. **214**, 405 (2002); H. Ebel, L.-I. Mielsch, and S. Bornholdt, Phys. Rev. E **66**, 035103(R) (2002).

Figure 1: Schematic diagram of the threshold model.

Figure 2: Numerical results for (a) $p(k)$, (b) $C(k)$, and (c) k_2/k using the networks of size $n = 50000$ generated by thresholding. The weight functions are taken to be exponential with $\lambda = 1$, $\theta = 10$ (crosses), logistic with $\beta = 1$, $\theta = 6$ (open squares) and $\beta = 1$, $\theta = 10$ (open circles), Gaussian (mean 0 and standard deviation 1.7) with $\theta = 6$ (closed squares), and Gaussian with $\theta = 10$ (closed circles). The theoretical predictions are shown for the exponential distribution (solid lines) and the logistic distributions (dotted lines).

Figure 3: Numerical results for (a) $p(k)$, (b) $C(k)$, and (c) k_2/k for the Pareto weight distributions with $n = 50000$ and $w_0 = 1$. We set $a = 0.5$, $\theta = 100$ (open squares), $a = 0.5$, $\theta = 500$ (open circles), $a = 1$, $\theta = 100$ (closed squares), and $a = 1$, $\theta = 500$ (closed circles). In (a), $p(k)$ estimated by Eq. (27) and the by power law approximation in Eq. (29) are also shown with solid lines and dotted lines, respectively.

Figure 4: Numerical results for (a) $p(k)$, (b) $C(k)$, and (c) k_2/k for the Cauchy weight distribution with $n = 50000$ with $\theta = 100$ (open squares), $\theta = 500$ (open circles), and the one-sided Cauchy distribution with $\theta = 100$ (closed squares), and $\theta = 500$ (closed circles). In (a), the analytically estimated $p(k)$ for the Cauchy distribution [Eq. (36)] and for the one-sided Cauchy distribution [Eq. (38)] are also shown by solid and dotted lines, respectively.

Figure 5: The evolution of (a) $p(k)$, (b) $C(k)$, and (c) k_2/k with the repetitive thresholding. We set $n = 50000$ and $\theta = 1$. The data shown are those after 1 (crosses), 8 (open squares), 10 (closed squares), 12 (circles), and 15 (triangles) rounds.

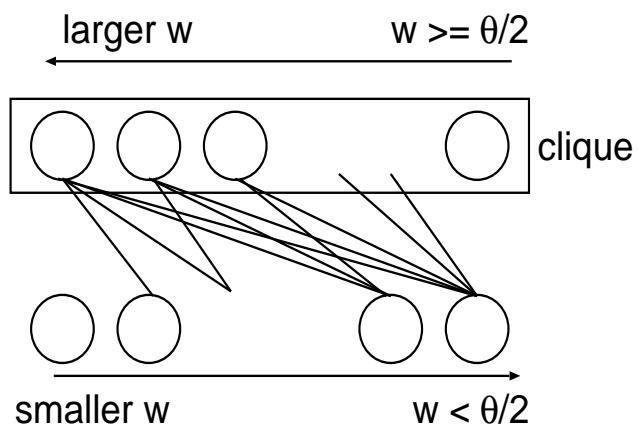


FIG. 1:

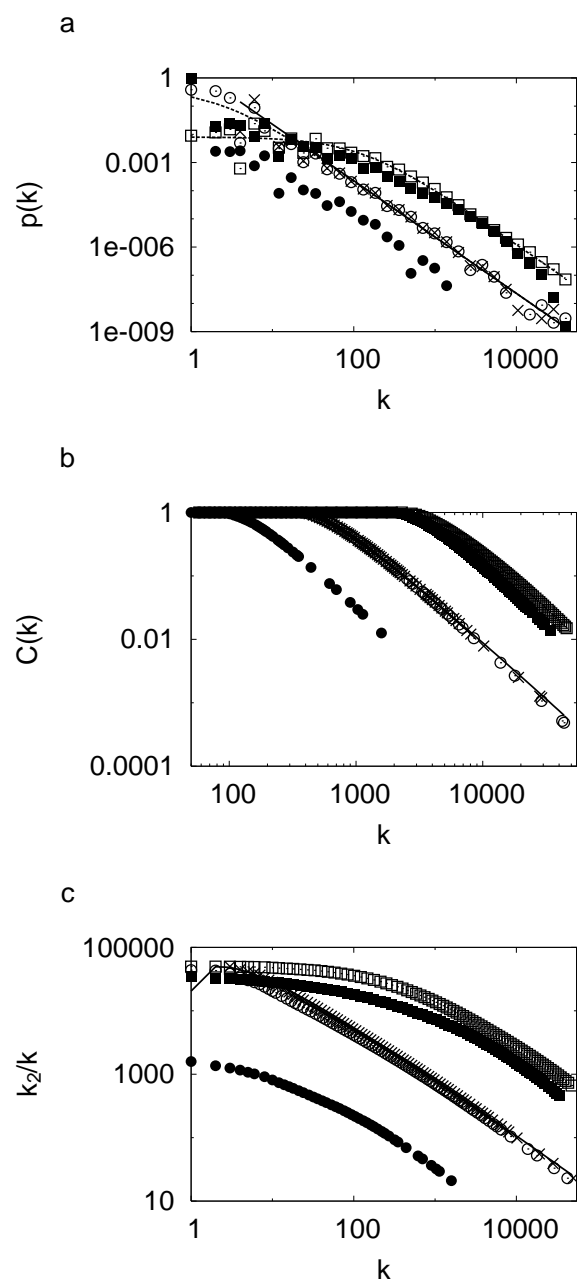


FIG. 2:

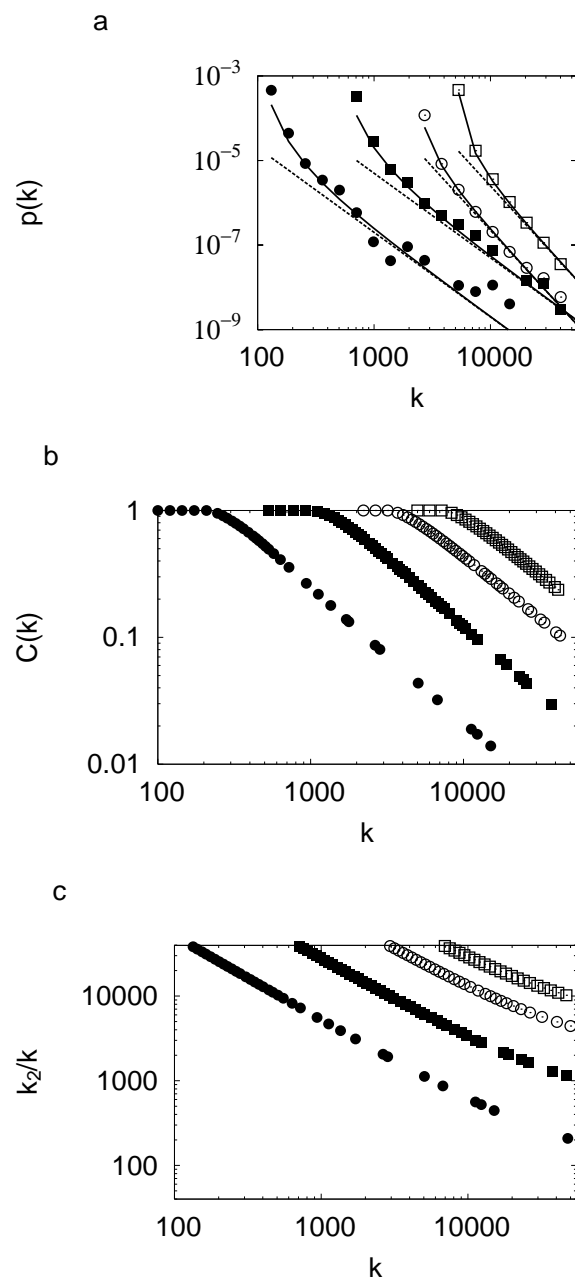
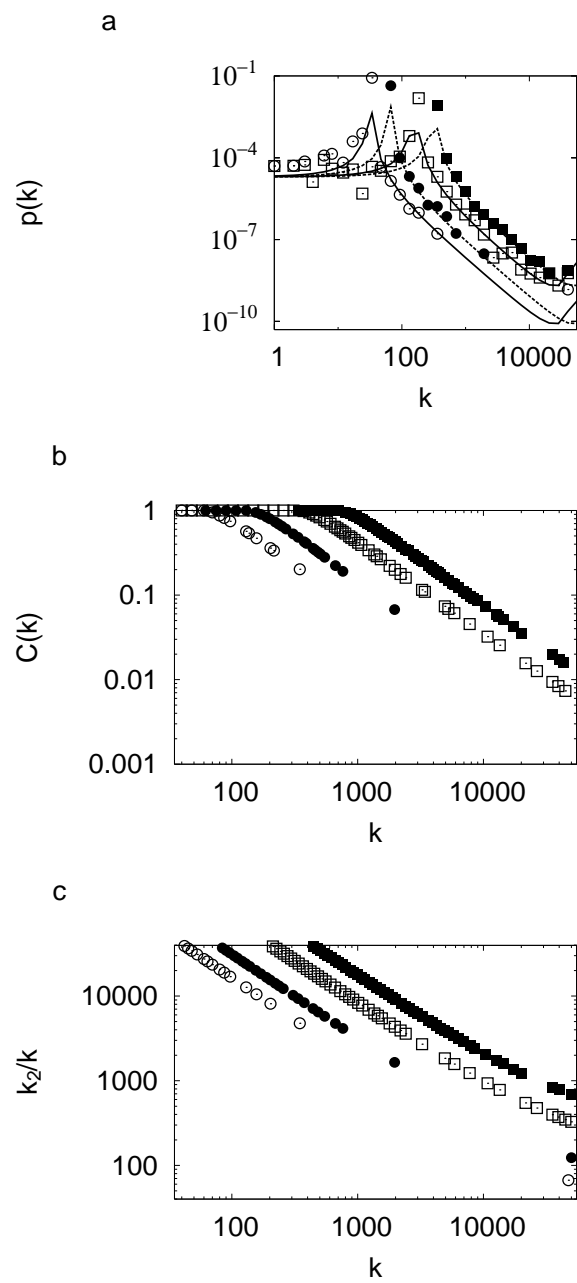


FIG. 3:



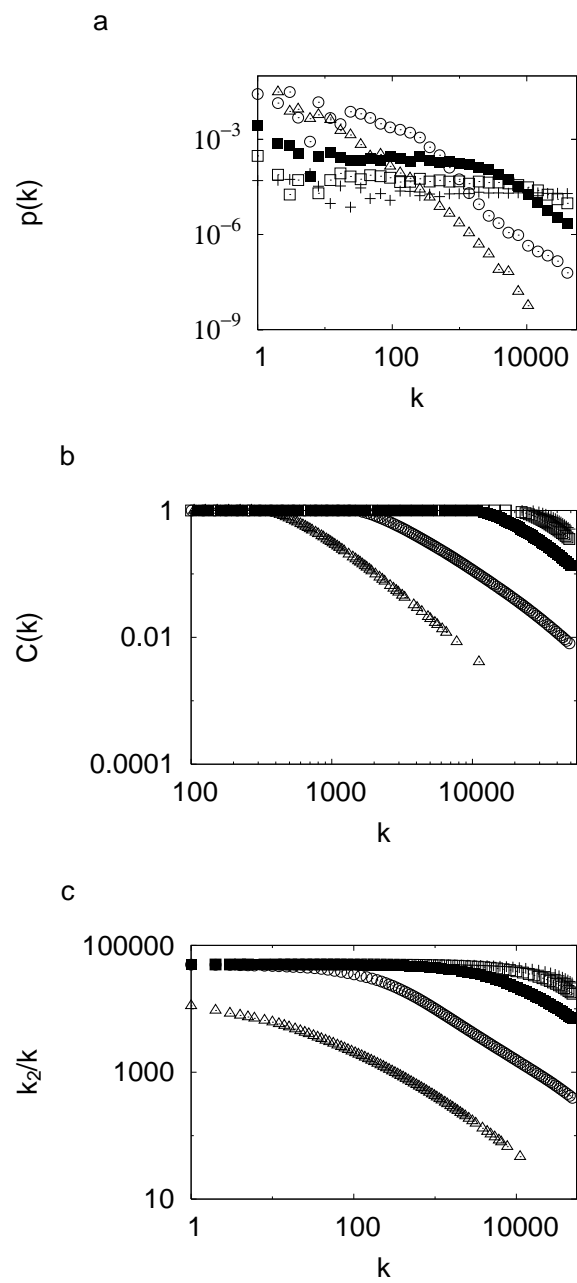


FIG. 5: